

THERMODYNAMIC SIMULATION OF HIGH TEMPERATURE, INTERNAL REFORMING FUEL CELL SYSTEMS

José Alexandre Matelli

Federal University of Santa Catarina
Mechanical Engineering Department
Campus Universitário
88040-900 Florianópolis, SC
matelli@cet.ufsc.br

Edson Bazzo

Federal University of Santa Catarina
Mechanical Engineering Department
Campus Universitário
88040-900 Florianópolis, SC
ebazzo@emc.ufsc.br

Abstract. This work presents a methodology for simulation of fuel cells to be used in power production in small on site power/cogeneration plants using natural gas. The methodology contemplates thermodynamics and electrochemical aspects related to molten carbonate and solid oxide fuel cells (MCFC and SOFC, respectively). Internal steam reforming is considered for hydrogen production. From inputs as cell potential, cell power, number of cell in the stack, ancillary systems power consumption, reformed natural gas composition and hydrogen utilization factor, the simulation gives the natural gas consumption, anode and cathode stream gases temperature and composition, and thermodynamic, electrochemical and practical efficiencies. Both energetic and exergetic methods are considered for performance analysis. The results obtained from natural gas reforming thermodynamics simulation show that the hydrogen production is maximum around 700 °C, for a steam/carbon ratio equal to 3. The fuel cells thermodynamic simulation results indicate that the SOFC is more efficient than MCFC, which is in accordance with the literature.

Keywords. Fuel cell, MCFC, SOFC, Natural gas reforming, Hydrogen

Nomenclature

\dot{E}_x	Exergy transfer rate (kW)	\dot{W}	Power output; Work transfer rate (kW)
F	Faraday's constant ($9,64867 \times 10^7$ C/kmol)	X	Molar fraction
G	Gibbs' free energy (kJ)	\bar{c}_p	Specific heat (kJ/kmolK)
\dot{I}	Irreversibility transfer rate (kW)	\bar{e}	Specific exergy (kJ/kmol)
H	Enthalpy (kJ)	\dot{m}	Mass flow (kg/s)
LHV	Lower heating value (kJ/kg)	n	Mole number
N	Number of cells in a stack	\dot{n}	Molar flow (kmol/s)
P	Pressure (kPa)	\bar{h}	Specific enthalpy (kJ/kmol)
Q	Heat (kJ)	\bar{s}	Specific entropy (kJ/kmolK)
\dot{Q}	Heat transfer rate (kW)		GREEKS
\bar{R}	Universal gases constant (8,31434 kJ/kmolK)	ε	Cell voltage (V)
S	Entropy (kJ/K)	ϕ	Hydrogen utilization factor
T	Absolute temperature (K)	η	Efficiency (%)
U	Internal energy (kJ)	λ	Steam-carbon rate
V	Volume (m ³); Electrode potential (V)	ξ	Standard chemical exergy (kJ/kmol)
W	Work (kJ)	ψ	Rational efficiency (%)

1. Introduction

In the current worldwide energetic scenario, fuel cells are presented as an emergent technology for power production. They are devices that convert the chemical energy of a fuel directly to power through an electrochemical process that has no relation with the Carnot's cycle and its efficiency. Thus the efficiency of a fuel cell is comparatively higher than the efficiency of a conventional thermodynamic cycle (the Rankine cycle, for instance) and reaches values as high as 45%. Depending on their characteristics, fuel cells can be used either in small on site power/cogeneration plants or as a power source for vehicles. In most cases, the fuel uses hydrogen and oxygen as oxidizing agent.

The major advantages of fuel cells are high efficiency, low on site emissions, clean and quiet operation, modularity and fast load response. In the other hand, the costs are very high and obtaining the hydrogen is not a trivial task. Despite

the disadvantages, fuel cells are considered a promising alternative to power production within a sustainable and clean energy production context.

This work presents a methodology for fuel cells thermodynamic simulation. Two types of fuel cells are analysed: MCFC (**M**olten **C**arbonate **F**uel **C**ell) and SOFC (**S**olid **O**xide **F**uel **C**ell). Their high operation temperature, 650 and 900°C, respectively, characterizes these kinds of cells. Internal steam reforming of natural gas, that is, the reforming reaction occurring inside the fuel cell anode, is considered in hydrogen production. The fuel cells are simulated in order to evaluate and compare their respective energetic, exergetic and environmental performances, based on the amount of CO₂ emissions.

2. Fuel cell system description

The fuel cells considered in this work are MCFC and SOFC, to be used in a 900 kW_{el} natural gas on-site power plant, as one can see in Figs (1) and (2). Both fuel cells operate with internal reforming of natural gas.

In the MCFC system illustrated in Fig. (1), natural gas (point 1) and water (point 9) are admitted into the double heat exchanger to pre-heat the gas stream and to generate steam. The pre-heated natural gas (point 2) and the steam (point 10) flow to the reforming chamber in the anode side of the fuel cell (point 3), where the steam reforming reaction occurs while the hydrogen produced in the reforming is consumed in the electrochemical reaction. Since MCFC are not sensitive to the presence of CO in the H₂ stream, no CO removing treatment is required. The heat associated to the combustion of the synthesis gas leaving the anode (point 4) in the combustion chamber (with additional air from point 5) is recovered in the heat exchanger. The system is adjusted such that the energy associated to the exhaust gases leaving the combustion chamber (point 6) is exactly sufficient to the gas pre-heating and steam production. The required temperature is guaranteed by the amount of air (point 5) supplied to the combustion reaction. The oxygen contained in the exhaust gases from the combustion chamber (point 7) is used in the cathode to complete the electrochemical reaction, and the resulting exhaust gases are rejected to the ambient. Water is also used in the cathode cooling system (points 11 and 12).

The SOFC system illustrated in Fig. (2) is similar to the MCFC system, except that in the SOFC system the heat exchanger is placed between the anode and combustion chamber.

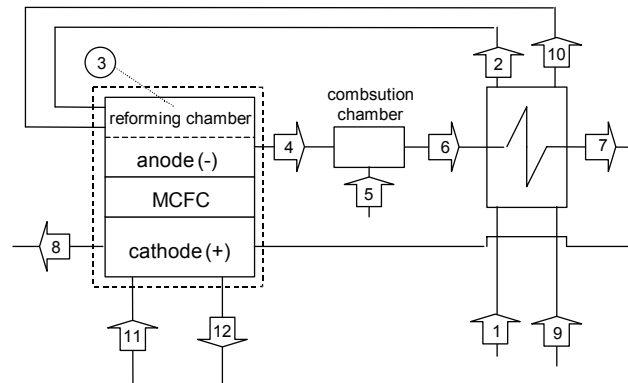


Figure 1. MCFC fuel cell system

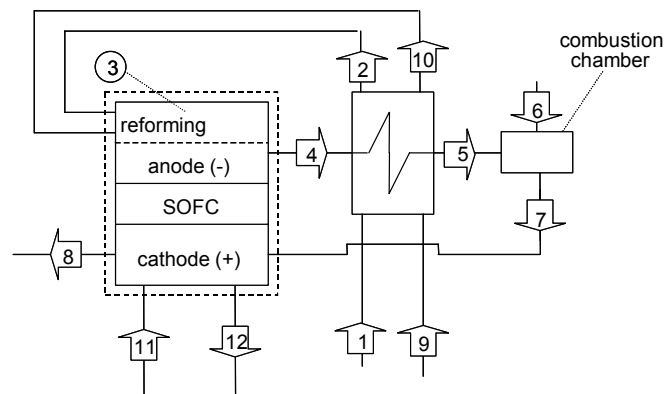


Figure 2. SOFC fuel cell system

3. Theoretical analysis of the fuel cell system

3.1. Thermodynamic analysis

Fuel cell is a device that converts the Gibbs free energy of a fuel directly into power. For convenience, this statement is demonstrated here for H₂-O₂ fuel cells, as shown in Fig. (3), considering the chemical reaction [Eq. (1)].

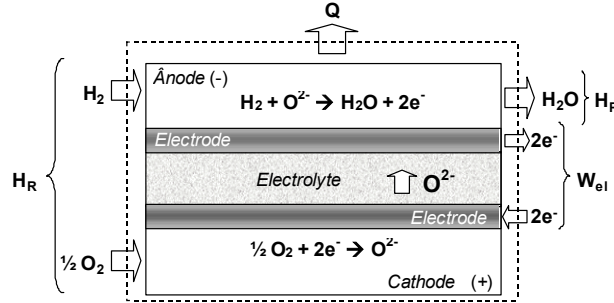


Figure 3. System for fuel cell analysis

Applying the 1st Law of Thermodynamics, neglecting kinetic and potential energy variations:

$$\delta Q - \delta W = dU \quad (2)$$

But,

$$dU = dH - PdV - VdP \quad (3)$$

Considering isobaric process and introducing Eq. (3) into Eq. (2), we have

$$\delta Q - \delta W = dH - PdV \quad (4)$$

Since in a fuel cell the reactions are electrochemical, the work in Eq. (4) is related to the work for the expansion of the gases plus the work due to the transport of electrical charges through the external circuit connecting the anode to the cathode. Thus,

$$\delta W = \delta W_{el} + PdV \quad (5)$$

If the process is considered reversible, the 2nd Law results in

$$\delta Q = TdS \quad (6)$$

The electrical work is obtained substituting Eq. (5) and Eq. (6) into Eq. (4) and rewriting, obtaining

$$\delta W_{el} = TdS - dH = -dG \quad (7)$$

As stated before, Equation (7) shows that the maximum net work is the Gibbs free energy obtained from the cell global reaction, Eq. (1), considering products and reactants at reference state (298,15 K e 101,3 kPa). Thus,

$$W_{el}^0 = -\Delta G^0 \quad (8)$$

The thermodynamic efficiency of a fuel cell is defined as the maximum work obtained in the cell divided by the energy released in the reversible isobaric global chemical reaction, as shown by Eq. (9)

$$\eta_{th} = \frac{\Delta G}{\Delta H} = 1 - \frac{T\Delta S}{\Delta H} \quad (9)$$

Therefore, it is clear that the thermodynamic efficiency of a fuel cell has no relation with the Carnot's cycle efficiency, because a fuel cell is an electrochemical device while a Carnot's engine is a thermal machine that operates between two heat reservoirs. A comparison between the efficiencies of a fuel cell and of a Carnot's engine is showed in Fig. (4).

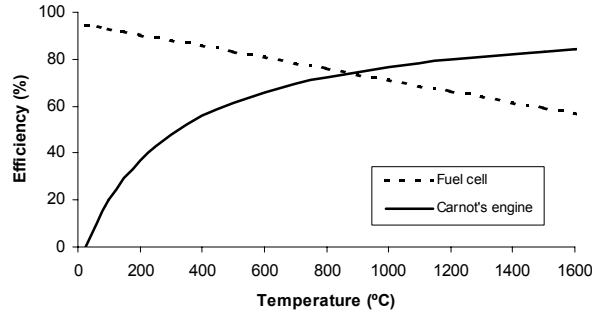


Figure 4. Comparison between the efficiencies of a fuel cell and a Carnot's engine (Kordesch and Simader, 1996).

3.2. Electrochemical analysis

The fuel cell electrical work (or its power output) can be written as a function of the difference of potential between the electrodes, as expressed in Eq. (10):

$$W_{el} = nF(V_{ct} - V_{an}) = nF\mathcal{E}_{cel} \quad (10)$$

Replacing Eq. (10) into Eq. (7), we have

$$\Delta G^0 = -nF\mathcal{E}_{cel}^0 \quad (11)$$

In the case of a H_2 - O_2 fuel cell [see Fig. (3)], the balance of charges requires that

$$n = 2 \cdot n_{H_2} \quad (12)$$

From Eq. (11), it follows that \mathcal{E}_{cel}^0 is the cell reversible potential, that is, the maximum possible difference of potential between the fuel cell electrodes. Since it is not possible to measure the potential of an isolated electrode, by convention the hydrogen electrode is adopted as the reference electrode, whose potential is set to zero. The potential values for several electrochemical reactions are listed in DeHoff (1993). Thus, for a fuel cell based in Eq. (1) the reversible potential is 1,229 V. However, several phenomena related to the kinetics of the electrochemical conversion in the electrodes introduce losses in the cell potential as the current intensity increases, as shown in Fig. (5). These losses are known as overpotential or overvoltage and their origin are not discussed in this work.

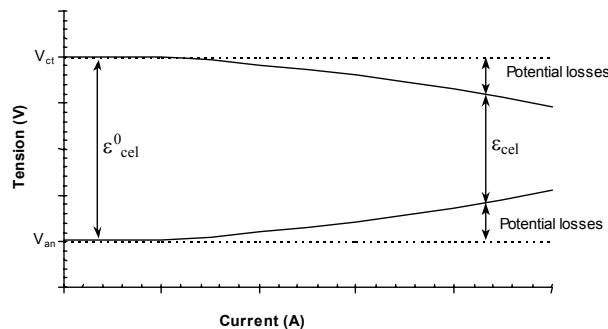


Figure 5. Potential losses in a fuel cell

The overpotential effects can be quantified through the *electrochemical efficiency*, defined as the real voltage of a cell divided by its maximum voltage, as showed by Eq. (13).

$$\eta_{elq} = \frac{\mathcal{E}_{cel}}{\mathcal{E}_{cel}^0} = \frac{W_{el}}{W_{el}^0} \quad (13)$$

Equation (13) can also be used to measure the quality of a fuel cell. Different technical projects of fuel cells, operating with the same reaction and with the same enthalpy, may present different electrochemical efficiency. Values as high as 90% for the electrochemical efficiency can be reached in H₂-O₂ fuel cells (Kordesch and Simader, 1996). Since the power output of a cell is equal to the voltage times its current, the maximum cell electrochemical efficiency – and also the *maximum cell thermodynamic efficiency* – occurs when the power output is zero, because $\mathcal{E}_{cel} = \mathcal{E}_{cel}^0$ when the current is zero, as one can see from Fig. (5).

The *practical efficiency* is defined as the real cell power output divided by the fuel enthalpy [see Eq. (26)], or as the thermodynamic efficiency multiplied by the electrochemical efficiency.

$$\eta_{prt} = \frac{W_{el}}{\Delta H} = \frac{nF\mathcal{E}_{cel}}{\Delta H} = \eta_{th} \cdot \eta_{elq} \quad (14)$$

For a fuel cell operating with hydrogen from natural gas reforming, the overall efficiency is associated to the total power output and the natural gas lower heating value. In this work, this efficiency is named 1st Law efficiency, and is given by

$$\eta_l = \frac{\dot{W}_{el}}{\dot{m}_{gn} LHV_{gn}} \quad (15)$$

3.3. Thermochemical aspects: natural gas reforming

Since hydrogen is not usually an energetic source abundantly available in its free form (as H₂ gas), it must be attained from other molecules. Among several methods of hydrogen obtaintion, the hydrocarbon reforming has been the most used, especially the methane reforming, due to its abundance in natural gas composition. Furthermore, the hydrogen concentration in the resulting stream gases is relatively high. This stream gas resulting from the reforming is named generically synthesis gas and its composition is typically H₂, CO, CO₂ and H₂O, and traces of other minor species. The exact composition depends on reforming type, temperature and pressure of reaction, steam/carbon ratio and catalyst. Among the methane reforming methods, the major three processes are the autothermal reforming, partial oxidation and steam reforming. (Ahmed and Krumpelt, 2001, Pulgar et al., 2002). The last one is considered in this work, whose global reforming reaction can be represented as



Steam reforming is a strongly endothermic reaction. Steam reacts with methane to produce CO, CO₂ and H₂. This process produces relatively high H₂ concentration (usually higher than 50%). The CO is undesirable in some types of fuel cells, like the proton exchange membranes PEM fuel cells, due to its poisoning potential of the electrolytic activity. It can be removed through several reactions, being the water-gas shifting reaction, showed in Eq. (17), the most common.



4. Performance analysis procedure

To determine the performance parameters, the energy and exergy balances are considered for a fuel cells system. Initially, the natural gas consumption or, specifically, the hydrogen from natural gas steam reforming consumption must be calculated. The hydrogen amount supplied to the anode depends on the equilibrium composition of the reforming reaction (Eq. 18), which is function of temperature, pressure and steam/carbon ratio, defined as the mole number of steam divided by the mole number of carbon in the fuel. Generically, we can represent as

$$X_{H_2,eq} = f(T, P, \lambda) \quad (18)$$

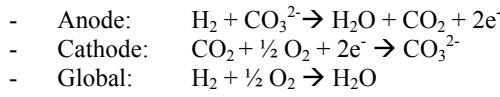
The method of element potentials (MEP) is used to find the equilibrium composition of reforming reaction. Using the Lagrange multipliers, the MEP finds the equilibrium point where the Gibbs free energy of the system is minimized, subject to the atomic population of the reactants. In this work, the MEP is used to simulate the natural gas steam reforming process, using the STANJAN Chemical Equilibrium Solver (Reynolds, 1987). It is considered that $P = 101,3 \text{ kPa}$, $\lambda = 3$ (Matelli, 2001) and a typical natural gas composition as presented in Tab. (1).

Table 1. Typical natural gas composition (Bazzo, 1995)

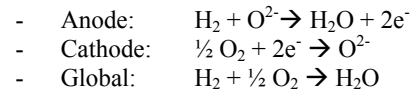
Component	Volumetric Fraction (%)	Mass Fraction (%)
CH ₄	90	82,2
C ₂ H ₆	6	10,3
N ₂	3	4,8
CO ₂	1	2,7

With the equilibrium composition of natural gas steam reforming, it is possible to simulate the fuel cells. The MCFC and SOFC electrochemical reactions are described below.

MCFC



SOFC



Both MCFC and SOFC operate at temperatures high enough to perform the steam reforming inside the anode. This process is known as *internal reforming*. The first step of the cell simulation is to determine the size of the stack, that is, how many cells must be serially connected to achieve the desired voltage and, consequently, the desired power output. In this work, we consider 992 cells for each stack, as suggested in Fig. (6). This value is obtained from commercially available phosphoric acid fuel cell (IFC, 2001). From cell voltage and power, the hydrogen consumption of electrochemical reaction is given by Eq. (19), re-written from Eq. (11).

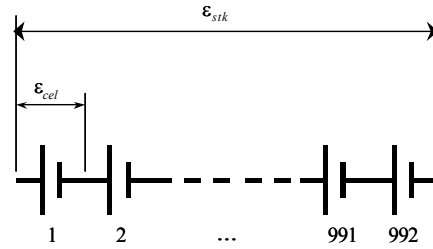


Figure 6. Scheme of a stack containing 992 cells

$$\dot{n}_{\text{H}_2, \text{cel}} = \frac{\dot{W}_{\text{cel}}}{2F\epsilon_{\text{cel}}} \quad (19)$$

The hydrogen consumption of each cell is a function of the hydrogen utilization factor, ϕ , defined as the ratio between the hydrogen amount which is consumed in the electrochemical reaction and the total amount of hydrogen which is supplied to the anode, as one can see in Eq. (20).

$$\phi = \frac{\dot{n}_{\text{H}_2, \text{cel}}}{\dot{n}_{\text{H}_2, \text{an}}} \quad (20)$$

The voltage of each type of cell is showed in Tab. (2), which values are found in the literature and also stated by manufacturers of functional prototypes. The hydrogen utilization factor is also presented in this table.

Table 2. ϵ and ϕ for each type of cell

Cell	ϵ (V)	ϕ
IRMCFC	0,6663	0,90
IRSOFC	0,6704	0,95

The stack hydrogen consumption is written as the sum of the consumption of each individual cell.

$$\dot{n}_{H_2,stk} = \sum_{i=1}^N n_{H_2,i} = N \cdot \dot{n}_{H_2,an} \quad (21)$$

The natural gas consumption of the stack is related to the hydrogen consumption through the steam reforming equilibrium composition, defined in Eq. (18).

$$\dot{n}_{gn,stk} = \frac{\dot{n}_{H_2,stk}}{X_{H_2,eq}} \quad (22)$$

In order to perform the energy balance in the stack (Fig. 7), it is necessary to know the enthalpies and entropies at the inlet and outlet stream gases. In this work, the stream gases are considered as perfect gases, which enthalpies and entropies are calculated according Eqs (23) and (24). In Eq. (24), the logarithm term is not considered, because it is very small when compared to other terms. The heat rejected is calculated from an energy balance, according to Eq. (25). A significative amount of the heat generated by the stack is absorbed by the reforming reaction and the several auxiliary control an environmental systems of the stack consume a part of the power produced.

$$\bar{h} = \sum_{j=1}^n X_j \left(\bar{h}_j^0 + \int_{T_0}^T \bar{c}_{p_j} dT \right) \quad (23)$$

$$\bar{s} = \sum_{j=1}^n X_j \left(\bar{s}_j^0 + \int_{T_0}^T \frac{\bar{c}_{p_j}}{T} dT - \bar{R} \ln X_j \right) \quad (24)$$

$$\dot{Q}_{ref} - \dot{Q}_{stk} + \dot{W}_{stk} - \dot{W}_{aux} = \sum \dot{n}_{out} \bar{h}_{out} - \sum \dot{n}_{in} \bar{h}_{in} \quad (25)$$

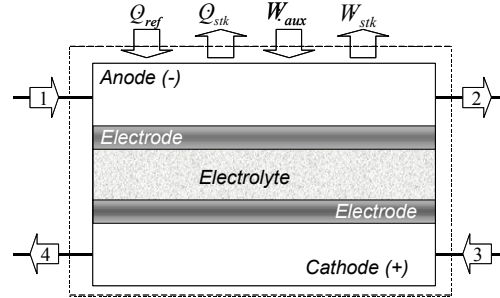


Figure 7. Energy balance

The thermodynamic, electrochemical and practical efficiencies are calculated from the Gibbs free energy, according to the following equations:

$$\Delta H_{stk} = \dot{n}_{H_2O,stk} \bar{h}_{H_2O} - \dot{n}_{O_2,stk} \bar{h}_{O_2} - \dot{n}_{H_2,stk} \bar{h}_{H_2} \quad (26)$$

$$\Delta S_{stk} = \dot{n}_{H_2O,stk} \bar{s}_{H_2O} - \dot{n}_{O_2,stk} \bar{s}_{O_2} - \dot{n}_{H_2,stk} \bar{s}_{H_2} \quad (27)$$

$$\Delta G_{stk} = \Delta H_{stk} - T_{cel} \Delta S \quad (28)$$

To complete the simulation, the energy, mass and exergy balances are performed in the combustion chamber and in the heat exchanger, according to:

$$\dot{Q} - \dot{W} = \sum \dot{n}_{out} \bar{h}_{out} - \sum \dot{n}_{in} \bar{h}_{in} \quad (29)$$

$$\sum \dot{m}_{in} = \sum \dot{m}_{out} \quad (30)$$

$$\dot{E}x_i^{\dot{Q}} - \dot{W} - \dot{I} = \sum \dot{n}_{out} \bar{e}_{out} - \sum \dot{n}_{in} \bar{e}_{in} \quad (31)$$

In Eq. (31), the exergies are calculated according to the following equations:

$$\dot{E}x^{\dot{Q}} = \dot{Q} \left(\frac{T - T_0}{T} \right) \quad (32)$$

$$\bar{e} = \bar{e}_{ph} + \bar{e}_{ch} \quad (33)$$

$$\bar{e}_{ph} = (\bar{h} - \bar{h}_0) - T_0 (\bar{s} - \bar{s}_0) \quad (34)$$

$$\bar{e}_{ch} = \sum_{j=1}^N X_j \xi_j + T_0 \bar{R} (X_j \ln X_j) \quad (35)$$

In Eq. (35), ξ_j is the standard chemical exergy of the j-th specie. In Tab. (3) are presented the values of ξ of the chemical species considered in this work.

Table 3. Standard chemical exergy (Kotas, 1984)

j	Specie	ξ (kJ/kmol)	j	Specie	ξ (kJ/kmol)
1	H ₂	238490	5	CH ₄	836510
2	CO	275430	6	C ₂ H ₆	1504360
3	CO ₂	20140	7	N ₂	720
4	H ₂ O	11710	8	O ₂	3970

The exergy balance leads to the concept of rational efficiency, defined as the ratio between the total outlet exergy and the total inlet exergy, according Eq. (36):

$$\psi = \frac{\Delta \dot{E}x_{out}}{\Delta \dot{E}x_{in}} = 1 - \frac{\dot{I}}{\Delta \dot{E}x_{in}} \quad (36)$$

The 2nd Law efficiency of a system is defined as the ratio between the useful power output and the fuel exergy, according Eq. (37). The fuel exergy is calculated from Eq. (35).

$$\eta_{II} = \frac{\dot{W}_{net}}{\dot{E}x_{fuel}} \quad (37)$$

Finally, the CO₂ emission is calculated based on the natural gas reforming reaction and natural combustion reaction (Eq. 38).



5. Results

The molar fractions found in the reforming reaction simulation are presented in Fig. (8). The hydrogen production reaches a maximum around 700 °C. Starting from 450 °C, the carbon monoxide production progressively increases. For temperatures higher than 700 °C, methane and ethane are completely reformed. The results obtained from the fuel cells simulations are showed in Table (4). The MCFC presented thermodynamic efficiency greater than the SOFC, because its operation temperature is smaller. This result is in accordance with the theoretical result presented in Fig. (4). In opposition, the SOFC presents electrochemical efficiency greater than the MCFC, because its voltage is greater, resulting in a smaller current for the same power output. Consequently, the overvoltage effects are smaller (see Fig. 3). The practical efficiency was found equal for both cell types. The SOFC has the 1st and 2nd Law efficiencies greater than

the MCFC, because its higher operation temperature allows a higher heat recovery in the reforming reaction, resulting in more hydrogen produced. The SOFC has also a greater rational efficiency than MCFC, because the temperatures and chemical species involved in its operation result in a smaller entropy generation. In Tabs. (5-8) are presented the results of the simulation for each point illustrated in Figs. (4) and (5). The pressure in all points were considered constant and equal to 101,3 kPa. The CO₂ emission is equal to 0,1234 kg/s for MCFC and equal to 0,1071 kg/s for SOFC.

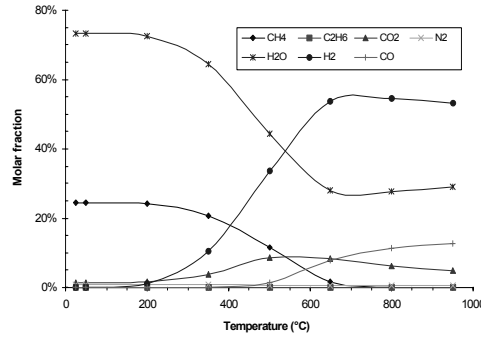


Figure 8. Molar fraction found for natural gas reforming simulation

Table 4. Results from fuel cells simulation

Fuel cell	T (°C)	ε_{stk} (V)	I (A)	\dot{W}_{stk} (kW)	\dot{W}_{aux} (kW)	ΔH (kW)	ΔS (kW/K)	ΔG (kW)	η_{th} (%)	η_{elq} (%)	η_{prt} (%)	η_l (%)	η_{II} (%)	ψ (%)
MCFC	650	661	1511	999	99	-1921	-0,4254	-1529	79,6	65,4	52,0	40,1	37,7	86,4
SOFC	900	665	1435	954	54	-1835	-0,4145	-1349	73,5	70,7	52,0	46,3	43,4	89,2

Table 5. MCFC system [see Fig. (1)]

Point	\dot{m} (kg/s)	\dot{n} (kmol/s)	MM (kg/kmol)	T (°C)	\bar{h} (kJ/kmol)	\bar{s} (kJ/kmolK)	\bar{e}_{ph} (kJ/kmol)	\bar{e}_{ch} (kJ/kmol)	\bar{e} (kJ/kmol)
1	0,04771	0,00272	17,52	25	-76398	189,3	0	842315	842315
2	0,04771	0,00272	17,52	100	-73512	197,9	316	842315	842631
3	0,1948	0,01591	12,25	650	-87853	197	9725	166910	176636
4	0,6611	0,02368	27,92	650	-256419	240,8	11869	43699	55568
5	0,7279	0,02523	28,85	25	0	194,3	0	429,5	429,5
6	1,389	0,04804	28,91	801	-126385	242,6	14804	5238	20042
7	1,389	0,04804	28,91	599	-134423	234,3	9235	5238	14473
8	0,9290	0,03639	25,53	576	-101905	227	8166	4063	12229
9	0,1471	0,00817	18,02	25	1889	6,61	0	11710	11710
10	0,1471	0,00817	18,02	100	48207	132,6	8752	11710	20462
11	0,6951	0,03858	18,02	25	1889	6,61	0	11710	11710
12	0,6951	0,03858	18,02	60	4526	14,97	144	11710	11854

Table 6. MCFC System – molar fractions [see Fig. (1)]

Point	X_{H_2} (%)	X_{CO} (%)	X_{CO_2} (%)	X_{H_2O} (%)	X_{CH_4} (%)	$X_{C_2H_6}$ (%)	X_{N_2} (%)	X_{O_2} (%)
1	0	0	1	0	90	6	3	0
2	0	0	1	0	90	6	3	0
3	54,26	7,810	8,137	27,60	1,680	0	0,5130	0
4	3,646	5,247	38,28	51,35	1,129	0	0,3447	0
5	0	0	0	0	0	0	79	21
6	0	0	22,01	28,22	0	0	41,49	8,281
7	0	0	22,01	28,22	0	0	41,49	8,281
8	0	0	7,707	37,26	0	0	54,78	0,256
9	0	0	0	100	0	0	0	0
10	0	0	0	100	0	0	0	0
11	0	0	0	100	0	0	0	0
12	0	0	0	100	0	0	0	0

Table 7. SOFC system [see Fig. (2)]

Point	\dot{m} (kg/s)	\dot{n} (kmol/s)	MM (kg/kmol)	T (°C)	\bar{h} (kJ/kmol)	\bar{s} (kJ/kmolK)	\bar{e}_{ph} (kJ/kmol)	\bar{e}_{ch} (kJ/kmol)	\bar{e} (kJ/kmol)
1	0,04139	0,00236	17,52	25	-76398	189,3	0	842315	842315
2	0,04139	0,00236	17,52	100	-73512	197,9	316	842315	842631
3	0,1690	0,01426	11,85	900	-71498	204,1	15748	164723	180471
4	0,2870	0,01426	20,12	900	-192700	239,5	17983	48489	66472
5	0,2870	0,01426	20,12	300,1	-216186	211,7	2768	49593	52362
6	0,6805	0,02359	28,85	25	0	194,3	0	128,4	128,4
7	0,9675	0,03672	26,35	609,4	-83971	229,3	8877	3078	11956
8	0,8476	0,03304	25,66	623,2	-94923	228,8	9256	3816	13073
9	0,1277	0,00709	18,02	25	1889	6,61	0	11710	11710
10	0,1277	0,00709	18,02	100	48207	132,6	8752	11710	20462
11	0,2172	0,01205	18,02	25	1889	6,61	0	11710	11710
12	0,2172	0,01205	18,02	60	4526	14,97	144	11710	11854

Table 8. SOFC system – molar fractions [see Fig. (2)]

Point	X_{H_2} (%)	X_{CO} (%)	X_{CO_2} (%)	X_{H_2O} (%)	X_{CH_4} (%)	$X_{C_2H_6}$ (%)	X_{N_2} (%)	X_{O_2} (%)
1	0	0	1	0	90	6	3	0
2	0	0	1	0	90	6	3	0
3	54,42	12,12	4,929	28,03	0,005	0	0,497	0
4	2,721	12,12	4,929	79,73	0,005	0	0,497	0
5	2,721	12,12	4,929	79,73	0,005	0	0,497	0
6	0	0	0	0	0	0	79	21
7	0	0	6,625	32,03	0	0	50,74	10,60
8	0	0	7,364	35,61	0	0	56,41	0,626
9	0	0	0	100	0	0	0	0
10	0	0	0	100	0	0	0	0
11	0	0	0	100	0	0	0	0
12	0	0	0	100	0	0	0	0

Conclusion

The methodology presented in this work is appropriated for performance analysis and to understand the thermodynamic behaviour of fuel cells. The thermochemical aspects related to the natural gas reforming were also taken into account. One of the major advantages of the present methodology is its step-by-step formulation, which makes it very easy to simulate in commercial solvers like the EES (Klein and Alvarado, 2001). The results obtained from natural gas reforming simulation show that the hydrogen production is maximum around 700 °C, and the carbon monoxide production progressively increases from 450 °C. The fuel cells simulations results indicate that the SOFC is more efficient than MCFC. The results found in this work are in good accordance with well-known parameters of fuel cells efficiency found in the literature.

References

- Ahmed, S., Krumpelt, M., 2001, "Hydrogen from hydrocarbons for fuel cells", Argonne National Laboratory, Electrochemical Technology Program, U.S.A., in International Journal of Hydrogen Energy, Vol. 26, pp 291-301.
- Bazzo, E., 1995, "Geração de vapor", 2ª Edição., Editora da UFSC, Florianópolis-SC.
- DeHoff, R. T., 1993, "Thermodynamics in material science", 1st edition, McGraw-Hill, New York, USA.
- Klein, S. A., Alvarado, F. L., 1992-2001, "Engineering Equation Solver", F-Chart Software, Middleton, USA.
- Kordesch, K. & Simader, G., 1996, "Fuel cells and their applications", 1st Edition, VCH Verlagsgesellschaft mbH, Weinheim, Federal Republic of Germany.
- Kotas, T. J., 1995, "The exergetic method of thermal plant analysis", Reprint Edition from the 1st Edition, Krieger Publishing Company, Malabar, Florida, USA.
- Matelli, J. A., 2001, "Sistemas de cogeração baseados em células-combustível aplicados em hospitais", Dissertação de mestrado, Universidade Federal de Santa Catarina, Florianópolis, 136 p.
- Pulgar, R. G., Matelli, J. A. and Oliveira, A. A. M., 2002, "Influence of natural gas reforming processes on the performance of a fuel cell", Proceedings of the 9th Brazilian Congress of Thermal Engineering and Sciences, Caxambu, Brazil.
- Reynolds, W. C., 1981-1987, "STANJAN.Chemical Equilibrium Solver", Department of Mechanical Engineering, Stanford University, USA.